Supporting Information

Enhancement of lattice dynamics by azimuthal plasmon on the femtosecond time scale in multi-walled carbon nanotubes

Dingguo Zheng[1,2], Siyuan Huang[1,2], Chunhui Zhu[1], Zhongwen Li[1], Yongzhao Zhang[1,2], Dong Yang[1], Huanfang Tian[1], Jun Li[1], Huaixin Yang[1,2,3], and Jianqi Li[1,2,3]*

[1]Beijing National Laboratory for Condensed Matter Physics, Institute of Physics, Chinese Academy of Sciences, Beijing, 100190, China

[2]School of Physical Sciences, University of Chinese Academy of Science, Beijing, 100049, China

[3]Yangtze River Delta Physics Research Center Co., Ltd., Liyang, Jiangsu, 213300, China

*Corresponding author: ljq@aphy.iphy.ac.cn

Calculation of MWCNT contraction

It is assumed that the photon-generated free electrons distribute homogeneously along the one-dimensional tubular structure. Then the linear charge density can be calculated by

$$\sigma = \frac{Q}{L} = \pi\left(R^2 - r^2\right)n_e e, \quad (1)$$

where $Q = \pi L\left(R^2 - r^2\right)n_e e$ is the total charge of the free electrons in nanotube; R, r, and L are the outer radius, inner radius, and length of the multiwalled nanotube, respectively; and n_e is the free electron density. Assume the average effective distance of each carbon atom away from a linear distributed charge is R. Then the average electric field applied on each carbon atom in the nanotube can be calculated by

$$E = \int_{-L/2}^{L/2} \frac{\sigma dl}{4\pi\varepsilon\left(R^2 + l^2\right)} \approx \frac{\sigma}{4\varepsilon R}, \quad (2)$$

where $\varepsilon = 4.5\varepsilon_0$ is the dielectric constant of the MWCNT for optical polarization perpendicular tubular axis[1]. Substituting equation (1) into (2), the average electric field inside the nanotube can be expressed as

$$E = \frac{\pi\left(R^2 - r^2\right)}{4\varepsilon R}n_e e. \quad (3)$$

The average coulomb force per carbon atom can be calculated by

$$F = eEf, \quad (4)$$

where $f = \frac{n_e}{n}$ is the efficiency of electron excitation, and n is carbon atom density in the nanotube, which is calculated to be 1.1×10^{23} cm^{-3} (C-C bond length is 1.42 Å, inter-layer distance is 3.4 Å, so a carbon atom occupies a space with 8.9×10^{-24} cm^3).

The photon-generated free electron density is estimated to be 2×10^{20} cm^{-3} [2] under a photon density of 6.5×10^{16} cm^{-2} (fluence ~25 mJ/cm^2, pulse width ~50 fs). Our MWCNTs R = 7 nm and r = 4 nm and using equations (3) and (4), we get an average electric field of ~3.0 GV/m inside the nanotube and an average force of ~9.5×10^{-13} N per carbon atom along the radial direction. Each carbon atom occupies an area of 2.62

Å^2 in nanotube; therefore, a pressure of ~36 MPa applied in radial direction of nanotube.

The Young's modulus of MWCNTs in the radial direction can be estimated based on the experimental results for graphite along the c-axis, 36.5 GPa [3,4]. Therefore, a pressure of ~36 MPa could induce a ~0.1% contraction along the radial direction for the MWCNTs.

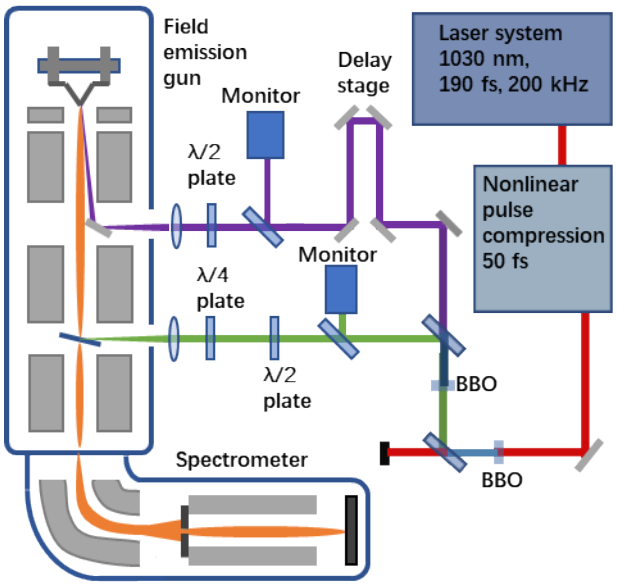

Fig. S1. Schematic illustration of the ultrafast TEM apparatus. The laser pulses are compressed to 50 fs by spectral broadening in a multi-pass cell, then the beam propagates through two β-barium borate (BBO) crystals for frequency doubling or quadrupling. The frequency-quadrupled beam (257 nm, purple) passes through the laser port and is reflected by an aluminum mirror, focusing on the TEM emitter [W (tungsten) tip] to emit electron pulses. The frequency-doubled laser beam (515 nm, green) is used to pump the sample. Two monitors ensure the stability of the laser beam. The light polarization is controlled using half-wave and quarter-wave plates. Electrons emitted from the tungsten filament are accelerated to 200 keV, then interact with sample and enter the spectrometer for EELS analysis and PINEM imaging (orange). The delay

times between the pump laser and electron probe are controlled by a delay stage in the frequency-quadrupled laser path.

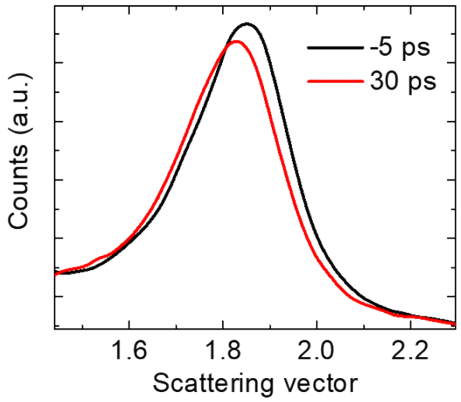

Fig. S2. Ultrafast diffraction peaks of the (002) reflection, taken 5 ps before (black) and 30 ps after (red) femtosecond laser excitation. The peaks in this 1D profile, which come from integrated along the radial direction in the 2D pattern, show a shift and intensity decrease after laser pumping. The optical polarization is parallel to the nanotube axis.

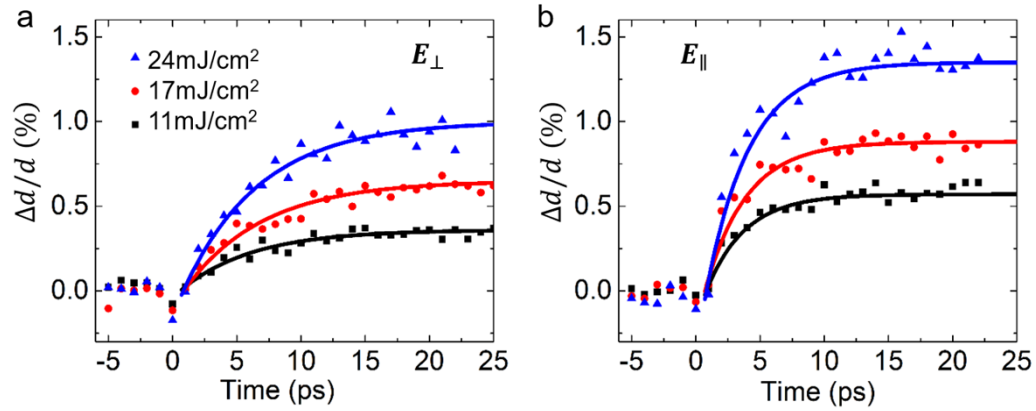

Fig. S3. Laser power dependent inter-layer structure evolution for light polarizations perpendicular (a) and parallel (b) to the nanotubes. Both for $E_\perp$ excitation and $E_\parallel$ excitation, the amplitudes of lattice expansion increase almost linearly with laser power. It is demonstrated that the different lattice expansions appear in the ps-time scale due to anisotropic optical absorption. On the other hand, the visible lattice contractions are commonly observed for optical excitation as light field perpendicular to the tubular axis.

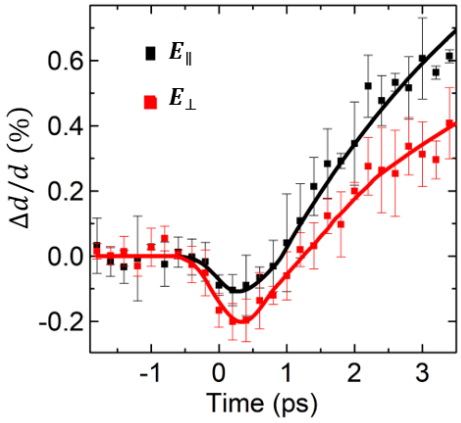

Fig. S4. Interlayer structural evolution clearly shows the lattice contraction in the fs-time scale.

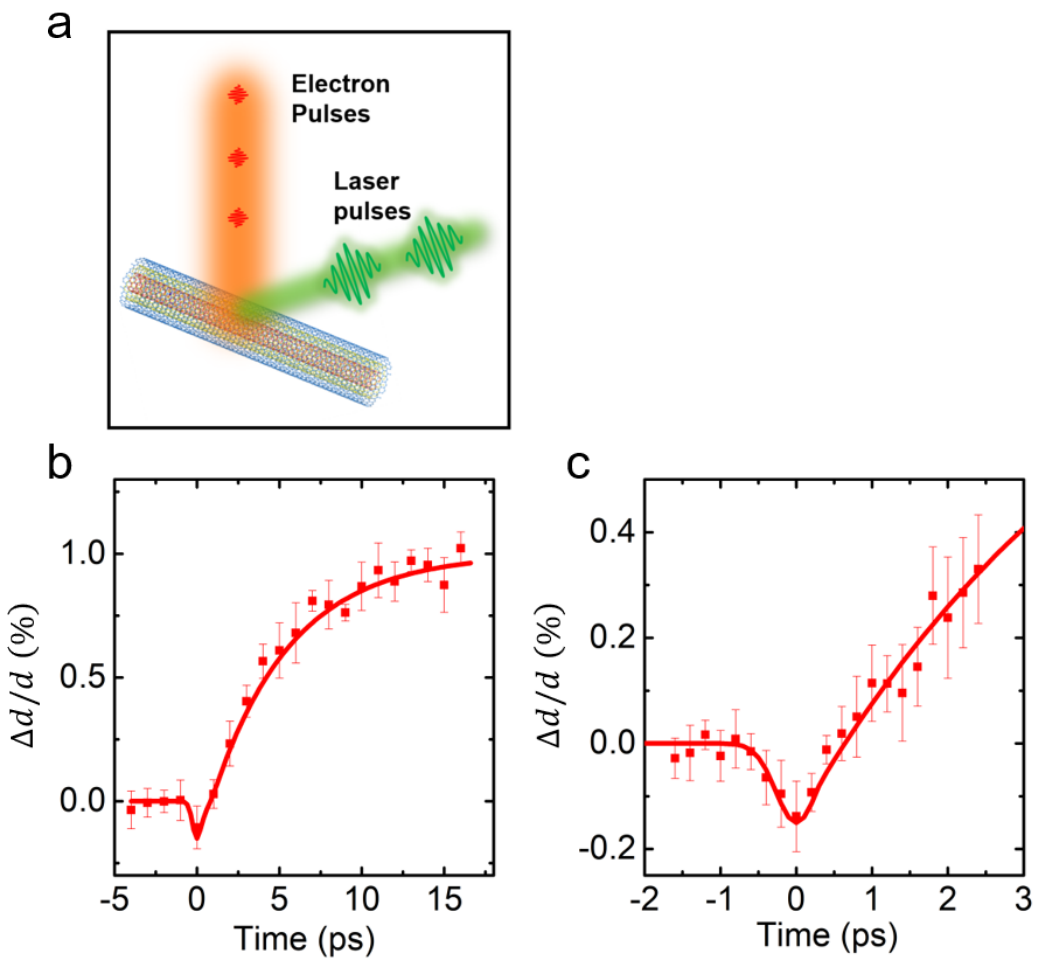

Fig. S5. The experimental data for interlayer distances change along the external electric field direction at a fluence of about 23 mJ/cm^2. (a) The experimental configuration shows that the laser beam has an angle with electron beam about 65° and the polarization is parallel to horizontal plane. Sample is tilted about 20° with the horizontal plane. (b) The interlayer distance changes in the ps-time time scale. (c) Experimental result shows the interlayer contraction.

1 S.-L. Chen, C.-C. Yu, S.-W. Chang, Y.-C. Lee, and H.-L. Chen, Optimization and Simulation of a Carbon Nanotube Arrangement for Transparent Conductive Electrodes with Record-High Direct Current to Optical Conductive Ratios. Opt. Mater. Express 11

(4), 1205 (2021).

2 M. C. Beard, J. L. Blackburn, and M. J. Heben, Photogenerated Free Carrier Dynamics in Metal and Semiconductor Single-Walled Carbon Nanotube Films. Nano Lett. 8, 4238 (2008).

3 J.-L. Tsai, S.-H. Tzeng, and Y.-T. Chiu, Characterizing elastic properties of carbon nanotubes/polyimide nanocomposites using multi-scale simulation. Composites Part B 41, 106 (2010).

4 O. L. Blakslee, D. G. Proctor, E. J. Seldin, G. B. Spence, and T. Weng, Elastic Constants of Compression-Annealed Pyrolytic Graphite. J. Appl. Phys. 41, 3373 (1970).